Available online at www.sciencedirect.com

SciVerse ScienceDirect

Ceramics International 38 (2012) 4453–4460

CERAMICS INTERNATIONAL

www.elsevier.com/locate/ceramint

Iron and chromium doped perovskite ($CaMO_3$ M = Ti, Zr) ceramic pigments, effect of mineralizer

C. Gargori, S. Cerro, R. Galindo, A. García, M. Llusar, G. Monrós *

Dpt. of Inorganic and Organic Chemistry, Jaume I University, Av. de Vicent Sos Baynat, s/n 12071, Castellón, Spain

Received 10 January 2012; received in revised form 7 February 2012; accepted 7 February 2012
Available online 15 February 2012

Abstract

Solid solutions $Ca(D_xM_{1-x})O_3$ (M = Ti, Zr and D = Fe,Cr), have been studied as ceramic pigment in conventional ceramic glazes using 0.5 mol/mol of NH_4Cl as flux agent by solid state reaction and by ammonia coprecipitation route. $Ca(Cr_xTi_{1-x})O_3$ compositions obtained without addition of NH_4Cl as mineralizer, produce pink color in glazes at low x but $CaCrO_4$ crystallizes when x increases, producing undesired green colors. The crystallization of chromates can be avoided using NH_4Cl as mineralizer, giving a complete solid solution that produce pink color in glazes at low x and dark blue shades at high x. Coprecipitated sample produce blue colors at low x and at low temperature than ceramic sample (1000 °C instead 1200 °C for CE sample). Cr^{4+} ion acts as red chromophore, but at higher x values (blue samples) Cr^{3+} ion entrance affects the color. $Ca(Fe_xTi_{1-x})O_3$ system crystallizes perovskite $CaTiO_3$ and pseudobrookite Fe_2TiO_5 together with rutile as residual crystalline phase, glazed samples change from a yellow to a pink color associated to the increase of pseudobrookite with firing temperature. $Ca(Fe_xTi_{1-x})O_3$ and $Ca(Cr_xZr_{1-x})O_3$ systems crystallize perovskite $CaZrO_3$ and zirconia (ZrO_2) in both monoclinic and cubic polymorphs, but iron or chromium oxides are not detected in the powders. Coprecipitated sample stabilises cubic form. The solid solution is not reached completely in these samples and is not stable in glazes.

Keywords: D. Perovskite; Ceramic pigment; Iron; Chromium

1. Introduction

Perovskite is a ceramic structure that would be added to CPMA list of ceramic pigments [1] because it is well known for its application as ceramic pigment since Eppler [2] developed black pigments from (Sr,Ca)MnO_3 perovskites using oxides and carbonates, mixed with conventional mineralizers fired at 730 °C with soaking time of 3 h. Other perovskites as neodymiates and titanates can be used as ceramic pigments [3,4]. Perovskite ABO_3 is an ideally cubic phase, but really becomes a rhombic syngony (space group Pnma): the A cation (Ca^{2+}, Sr^{2+}, Cd^{2+}, Ba^{2+}, Ni^{2+}, Co^{2+}) ideally occupies vertex of cube and the B cation (Ti^{4+}, Zr^{4+}, Sn^{4+}) the centre, oxygens occupy face centres.

Chromium and iron act as chromophore agents in several ceramic pigments listed by DCMA [1]: pink of chromium–alumina $(Al,Cr)_2O_3$ (3–03–5), green chromium hematite Cr_2O_3 (3–05–3), green victoria garnet $Ca_3Cr_2Si_3O_{12}$ (4–07–3), several chromium-rutile pigments $(Cr,M\cdot Ti)O_2$ M = Sb, Nb, W or Mn (11–17–16, 11–18–6, 11–19–6 and 11–46–7), several chromium-spinel pigments $A(B,Cr)_2O_4$ (13–29–2, 13–30–3, 13–32–5, 13–33–7, 13–37–713–38–9, 13–40–9, 13–48–7, 13–50–9 and 13–51–7) in chromium case, and hematite brown (3–06–7), iron–chromium spinel brown (13–33–7), iron–titanium spinel brown (13–34–7), iron–nickel spinel brown (13–35–7), iron–zinc spinel brown (13–36–7), iron–zinc–chromium spinel brown (13–37–7), iron–cobalt spinel black (13–39–9), iron–cobalt–chromium spinel black (13–40–9), iron–manganese spinel black (13–41–9), iron–manganese–chromium spinel brown (13–48–7), iron–nickel chromium spinel black (13–50–9) and pink koral zircon (14–44–5) for iron.

Nine crystalline phases are stable at liquidus temperature in the system $CaO–Fe_2O_3–TiO_2$ under strongly reducing conditions [5]: (a) rutile (TiO_2, with some iron oxide in solid solution), (b) perovskite ($CaTiO_3$ solid solution), (c) ($Ca_4Ti_3O_{10}–Ca_3Ti_2O_7$) solid solution, (d) lime (CaO with iron oxide in solid solution), (e) pseudobrookite (Fe_2TiO_5 solid solution), (f) ilmenite ($FeTiO_3$ solid solution), (g) ulvospinel

---

* Corresponding author. Tel.: +34 0964 728250; fax: +34 0964 728214.
E-mail address: monros@qio.uji.es (G. Monrós).

doi:10.1016/j.ceramint.2012.02.019

(Fe_2TiO_4 solid solution), (h) wustite ($Fe_{1-x}O$ with calcium and/or titanium in solid solution) and (i) dicalciumferrite ($Ca_2Fe_2O_5$ solid solution). The study of mutual solubility of perovskite $CaTiO_3$ and ilmenite $FeTiO_3$ under strongly reducing conditions show that there is no appreciable solid–solution formation along the join $CaTiO_3$–$FeTiO_3$: in 4 wt.% of $FeTiO_3$–96 wt.% of $CaTiO_3$ binary system fired at 1280 °C and an atmosphere of $CO_2/CO = 0.291$, rutile and pseudobrookite are detected together perovskite, furthermore it is pointed out that ilmenite does not incorporate as much as 2 wt.% of perovskite under these experimental conditions.

Perovskite, $CaTiO_3$, shows mixed ionic and electronic conductivity at low oxygen partial pressure and maintains its structure in the presence of high concentrations of defects [6]. Substitution of calcium titanate by acceptor impurities in Ti-sites improves both ionic and electronic conductivity [7]. The most considerable increase of the electrical conductivity is achieved by iron substitution, which makes this material particularly attractive for use as a membrane for hydrogen production. The samples of the system $CaTi_{1-x}Fe_xO_{3-\delta}$ ($x = 0$, 0.1, …, 0.5) were synthesised by solid-state reaction of the corresponding oxides or carbonates by Dunyushkina [7]. These materials were weighed in the defined molar ratio and mixed in an agate mortar under ethyl alcohol for about 30–40 min. The homogeneous powders were pressed and heated at a rate of 5 °C/min to a temperature of 1200 °C where they were kept for 2 h. The fired pellets were ground again, pressed for the second time, heated at the same rate to 1470 °C and exposed for 2 h. According to X-ray diffraction analysis results all samples were single-phase and exhibited orthorhombic symmetry.

Murashkina and Demina study the $Ca(Cr_xTi_{1-x})O_{3-\delta}$ $x = 0.1$, 0.2, 0.3, 0.4 and 0.5 samples prepared by the conventional ceramic route, using extrapure-grade $CaCO_3$, TiO_2 and analytical-grade Cr_2O_3. Samples were precalcined at 500 °C for 2 h to remove adsorbed gases and moisture, then fired at 1200 °C in 5 h [8]. After regrinding in ethanol, the samples were pressed into pellets, which were then sintered at 1450 °C for 4 h. XRD examination indicated the formation as single phase of $Ca(Cr_xTi_{1-x})O_{3-\delta}$ solid solutions in the range $x = 0$–0.2 and samples $x = 0.3$, 0.4 and 0.5 showed additional reflections from $CaCrO_{3-\delta}$. The lattice parameters of the solid solutions decrease with increasing Cr content, as would be expected given that the ionic radius of Cr^{4+} (0.52 Å) is smaller than that of Ti^{4+}(0.68 Å). Perovskites possess high ionic–electronic conductivity and are stable in a broad range of oxygen partial pressures. At the same time, the oxygen ionic conductivity of undoped perovskite titanates is rather low. Partially substituted $Ca(M_xTi_{1-x})O_3$ titanates with M = 3d transition metal substitutions such as Fe, Al or Ga on the Ti site, increase the conductivity of calcium titanate. Theoretical analysis suggests that charge transport in such materials is due to oxygen vacancies and electrons. Their structural, chemical, and electrical properties can be varied over broad ranges by substituting various metals. The effects of different dopants on the electrical properties of calcium, strontium, and barium titanates have been studied extensively. The results indicate that partial substitution of acceptor ions on the Ti site increases the concentration of oxygen vacancies and, as a consequence, the conductivity of the material.

The authors have described the synthesis and characterization of both new ceramic pigments based on chromium–calcium titanate (red-pink) [9] and vanadium doped calcium titanate (orange), respectively [10]. The former pigment is based on the solid solution of chromium (IV) in $CaTiO_3$. When it is characterized as pigment in a CaO–ZnO–SiO_2 conventional transparent glaze used for ceramic tiles (1080 °C) produce the best red-brown color using 0.015 mol/mol of chromium and fired at 1100 °C with a soaking time of 3 h (5% weight added to the transparent glaze show CIEL*a*b* valours of 59.3/12.5/9.5). Likewise 5 wt.% addition of NH_4Cl used as flux agent increase a* and decrease both b* and L* valours (L*a*b* = 45.2/15.3/5.3).

In this paper the pigmenting capacity in conventional ceramic glazes of iron and chromium doped $CaMO_3$ M = Ti, Zr solid solutions, adding 0.5 mol/mol of NH_4Cl (m.p. 338 °C, decomposes) as mineralizer, have been studied.

2. Experimental

Iron and chromium doped $CaMO_3$ M = Ti, Zr solid solutions: $Ca(D_xM_{1-x})O_3$ $x = 0.2$, 0.4, 0.6 and 1 for D = Fe samples and $x = 0.025$, 0.05, 0.1 and 0.2 for D = Cr samples, with addition of 0.5 mol/mol of NH_4Cl as flux agent, has been prepared by both ceramic method (CE) and an alternative ammonia coprecipitation method (CO). In CE method, calcium carbonate $CaCO_3$, chromium oxide Cr_2O_3, iron oxide Fe_2O_3, anatase TiO_2 and NH_4Cl, all supplied by Panreac S.A., have been used as precursors to 20 g of final product. Ceramic mixture were milled in acetone medium, and dried at open air. In CO method, $Cr(NO_3)_3 \cdot 9H_2O$, $Fe(NO_3)_3 \cdot 9H_2O$, $Ca(NO_3)_2 \cdot 4H_2O$ and titanium isopropoxide, all supplied from Aldrich S.A., and NH_4Cl supplied by Panreac S.A., have been used as precursors to 10 g of final product. Nitrates were solved in 200 ml of water and maintaining 70 °C and continuous stirring, titanium isopropoxide was dropped to the solution, and then concentrated ammonia solution was dropped until pH 8 was reached. The coprecipitated was dried at 110 °C. Both CE and CO dried samples were fired at 1000 °C with 3 h of soaking time and after manually grinding in agate mortar, successively at 1200 °C with 3 h of soaking time also [11].

Samples have been characterized by several techniques:

(a) X-ray diffraction (XRD) carried out on a Siemens D5000 diffractometer using Cu Kα radiation, 20–70° 2θ range, scan rate 0.05° 2θ/s, 10 s per step and 40 kV and 20 mA conditions.
(b) Microstructure characterization of powders was carried out by scanning electron microscopy (SEM), using a Leo-440i microscope supplied by LEYCA.
(c) UV–vis–NIR spectra of 5% weight glazed samples in a conventional SiO_2–CaO–ZnO glaze for double firing stoneware have been collected using a Lambda 2000 spectrometer supplied by Perkin Elmer through diffuse reflectance technique. L*a*b* color parameters of, glazed

samples were measured following the CIE (Commission International de l'Eclairage) colorimetric method [12] using a Perkin-Elmer spectrophotometer, with standard lighting D65. On this method, L* is a measure of brightness (100 = white, 0 = black) and a* and b* of chroma (−a* = green, +a* = red, −b* = blue, +b* = yellow).

(d) Specific surface analyzer Gemini V equipped with Flow Prep 060 gas desorption system supplied by Micromeritics was used for specific surface measurements B.E.T. [13] of samples.

3. Results and discussion

XRD evolution of crystalline phases in ceramic samples and CIEL*a*b* parameters of powders and 5% glazed in a conventional CaO–ZnO–SiO_2 glaze in function of chromophore agent, temperature and synthesis method are shown in Tables 1–3. Representative XRD difractogrammes of powders are shown in Figs. 1–3. UV–vis–NIR spectra of powders fired at 1200 °C and 5 wt.% glazed in a conventional CaO–ZnO–SiO_2 glaze in function of chromophore agent, temperature and synthesis method are shown in Figs. 4–7.

3.1. *Chromium doped calcium titanate Ca(Cr$_x$Ti$_{1-x}$)O$_3$ without mineralizer*

XRD evolution of crystalline phases in ceramic powders Ca(Cr$_x$Ti$_{1-x}$)O$_3$ without mineralizer addition fired at 1000 °C/3 h and CIEL*a*b* parameters of 5% glazed powders in a conventional CaO–ZnO–SiO_2 glaze are shown in Table 1 and their corresponding difractogrammes in Fig. 1.

All ceramic powders Ca(Cr$_x$Ti$_{1-x}$)O$_3$ show pink color (L*a*b* ≈ 40/10/7), but 5 wt.% glazed in a conventional CaO–ZnO–SiO_2 glaze (1050 °C) produce pink color in samples $x = 0.05$ (L*a*b* = 56.1/7.6/6.8) and 0.1 (L*a*b* = 54.4/4.5/8.5), but turns to green color (L*a*b* = 60.6/−4.2/13.4 for $x = 0.3$) and produce profuse pin-hole defects in samples $x = 0.2$ and $x = 0.3$. XRD evolution of crystalline phases in Fig. 1 and Table 1 indicate that together perovskite sample crystallizes calcium chromate that produce pin hole when decompose and dissolves into molten glaze following the reaction:

$$2CaCrO_4 \rightarrow Cr_2O_3 + 2CaO + (3/2)O_2 \qquad (1)$$

The resulting chromium and calcium oxides in Eq. (1) dissolves in glaze producing the green color on glazed samples. In order to avoid the crystallization of chromates, as described in [9] the optimal pigmenting sample Ca(Cr$_x$Ti$_{1-x}$)O$_3$ $x = 0.015$ were modified by addition of 5 wt.% of three different flux

Table 1
XRD evolution of crystalline phases in ceramic powders Ca(Cr$_x$Ti$_{1-x}$)O$_3$ without mineralizer addition fired at 1000 °C/3 h and CIEL*a*b* parameters of 5% glazed powders in a conventional CaO–ZnO–SiO_2 glaze.

Ca(Fe$_x$Ti$_{1-x}$)O$_3$	$x = 0.05$	$x = 0.1$	$x = 0.2$	$x = 0.3$
L*a*b*	56.1/7.6/6.8	54.4/4.5/8.5	58/−2.3/11.8[a]	60.6/−4.2/13.4[a]
Crystalline phases	P(500)	P(350)T(10)	P(320)T(100)	P(300)T(400)

Crystalline phases: P(perovskite $CaTiO_3$ or $CaZrO_3$), T(calcium chromate $CaCrO_4$), peak intensity (c.p.s.) indicated between parenthesis for the selected peak: perovskite $CaTiO_3$ (33.2° 2θ), $CaCrO_4$(24.5° 2θ).

[a] Glazed sample shows a profuse pin-hole defect.

Table 2
XRD evolution of crystalline phases in powders $x = 0.2$ in function of chromophore agent, temperature and synthesis method.

Sample	T (°C)	Method	Crystalline phases
Ca(Fe$_{0.2}$Ti$_{0.8}$)O$_3$	1000	CE	P(400)R(25)B(70)
		CO	P(300)R(100)B(60)
	1200	CE	P(480)R(50)B(70)
		CO	P(300)R(150)B(70)
Ca(Cr$_{0.2}$Ti$_{0.8}$)O$_3$	1000	CE	P(400)R(20)
		CO	P(400)R(20)
	1200	CE	P(380)R(20)
		CO	P(400)
Ca(Fe$_{0.2}$Zr$_{0.8}$)O$_3$	1000	CE	P(500)M(200)Z(80)
		CO	P(400)M(20)Z(350)
Ca(Cr$_{0.2}$Zr$_{0.8}$)O$_3$	1000	CE	P(350)M(80)Z(700)
		CO	P(300)Z(800)

Crystalline phases: P(perovskite $CaTiO_3$ or $CaZrO_3$), R(rutile TiO_2), B(pseudobrookite Fe_2TiO_5), M(monoclinic ZrO_2), Z(cubic ZrO_2), peak intensity (c.p.s.) indicated between parenthesis for the selected peak: perovskite $CaTiO_3$ (33.2° 2θ), $CaZrO_3$(32° 2θ), rutile (27.5° 2θ), B pseudobrookite (25.5° 2θ), M monoclinic ZrO_2(25.5° 2θ), and cubic zirconia (30° 2θ).

Table 3
CIEL*a*b* parameters of $x = 0.2$ powders and 5 wt.% glazed in a conventional CaO–ZnO–SiO_2 glaze surfaces in function of chromophore agent, temperature and synthesis method.

Sample	T (°C)	Method	L*a*b*
Ca(Fe$_{0.2}$Ti$_{0.8}$)O$_3$	1000	CE powder	65/9/21
		CO powder	50/11/11
	1200	CE glazed	73/12/18
		CO glazed	**65/16/17**
Ca(Cr$_{0.2}$Ti$_{0.8}$)O$_3$	1000	CE powder	62/9/18
		CE glazed	74/10/28
		CO powder	49/9/12
		CO glazed	**51/2/−3**
	1200	CE glazed	49/3/−2
		CO glazed	**45/3/−3**
Ca(Fe$_{0.2}$Zr$_{0.8}$)O$_3$	1000	CE powder	67/8/28
		CE glazed	No color
		CO powder	60/6/19
		CO glazed	No color
	1200	CE powder	73/2/31
		CE glazed	No color
		CO powder	50/7/15
		CO glazed	No color
Ca(Cr$_{0.2}$Zr$_{0.8}$)O$_3$	1000	CE powder	45/10/9
		CE glazed	62/−1/13
		CO powder	54/5/10
		CO glazed	64/−1/14
	1200	CE powder	40/10/9
		CE glazed	61/−2/10
		CO powder	41/9/10
		CO glazed	63/−2/12

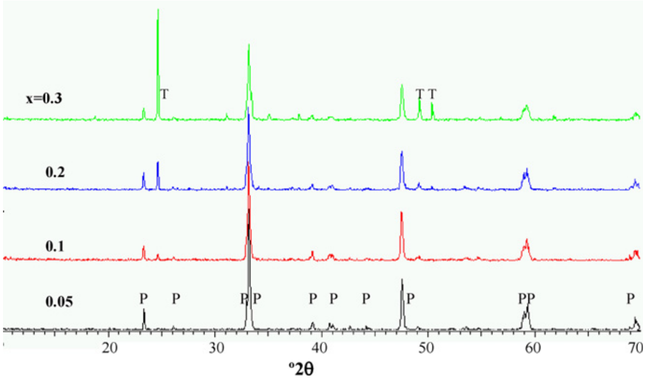

Fig. 1. XRD difractogrammes of CE ceramic powders $Ca(Cr_xTi_{1-x})O_3$ without mineralizer addition fired at 1000 °C: P(perovskite $CaTiO_3$), T(calcium chromate $CaCrO_4$).

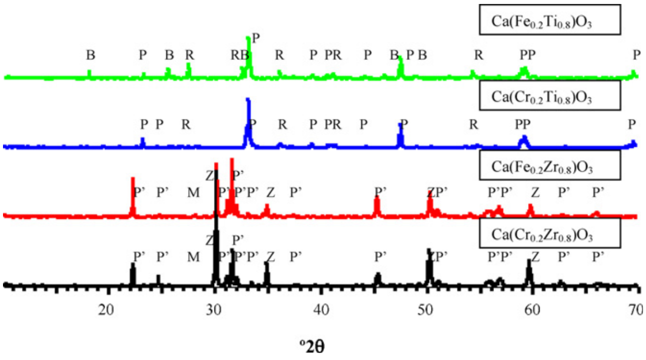

Fig. 2. XRD difractogrammes of CO powders fired at 1000 °C: P(perovskite $CaTiO_3$ or $CaZrO_3$), R(rutile TiO_2), B(pseudobrookite Fe_2TiO_5), M(monoclinic ZrO_2), and Z(cubic ZrO_2).

agents: $NaNO_3$ (m.p. 308 °C, b.p. 380 °C, decomposes), NH_4Cl (m.p. 338 °C, decomposes) and NaF (m.p. 993 °C). The CIEL*a*b* valours measured in 5 wt.% glazed samples fired at 1100 °C were 73.4/9.3/14.7 ($NaNO_3$), 55.6/13.9/9.6 (NaF) and 45.2/15.3/5.3 (NH_4Cl) respectively, indicating that NH_4Cl mineralizer increase significantly the red shade (a* = 15.3) and also the color intensity (L* = 45.2). The interesting result obtained using NH_4Cl is applied now in order to study the possibility of higher entrance of chromium in perovskite $Ca(Cr_xTi_{1-x})O_3$ solid solution avoiding chromates crystallization.

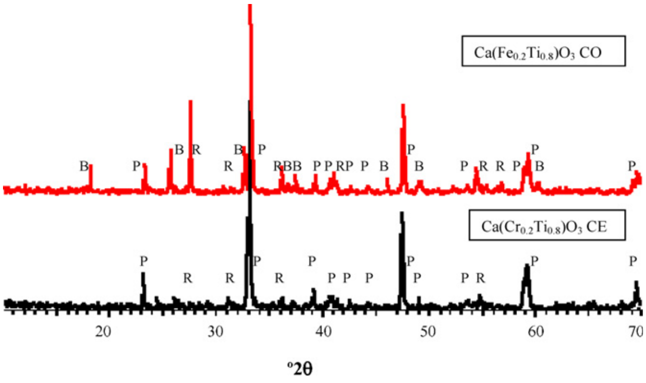

Fig. 3. XRD difractogrammes of indicated powders fired at 1200 °C.

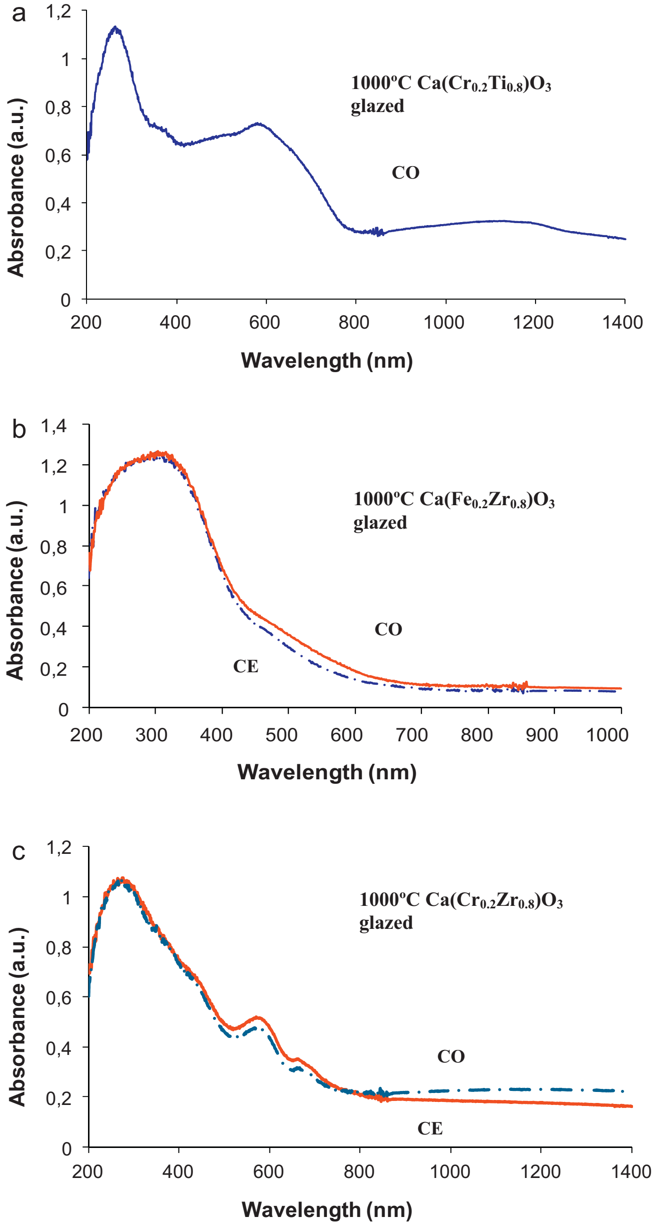

Fig. 4. UV–vis–NIR spectra of indicated glazed samples of powders fired at 1000 °C.

3.2. Chromium doped calcium titanate $Ca(Cr_xTi_{1-x})O_3$ with addition of 0.5 mol/mol of NH_4Cl

XRD results indicate that $Ca(Cr_xTi_{1-x})O_3$ $x = 0.2$ CE and CO samples crystallize perovskite $CaTiO_3$ and rutile as residual phase at 1000 °C (Table 2 and Fig. 2). At 1200 °C perovskite is the only crystalline phase detected in CO sample and, when x increase (Table 4), only perovskite is detected, but the color of glazed samples change from a red-pink shade at low x (L*a*b* = 46/14/2 for CO $x = 0.025$ sample) [9], to a dark blue color for $x = 0.1$ and 0.2 samples, decreasing both a* and b* parameters (L*a*b* = 45/3/−3 for CO sample $x = 0.2$). At 1000 °C, only CO $x = 0.2$ sample produce blue shade (see Table 3).

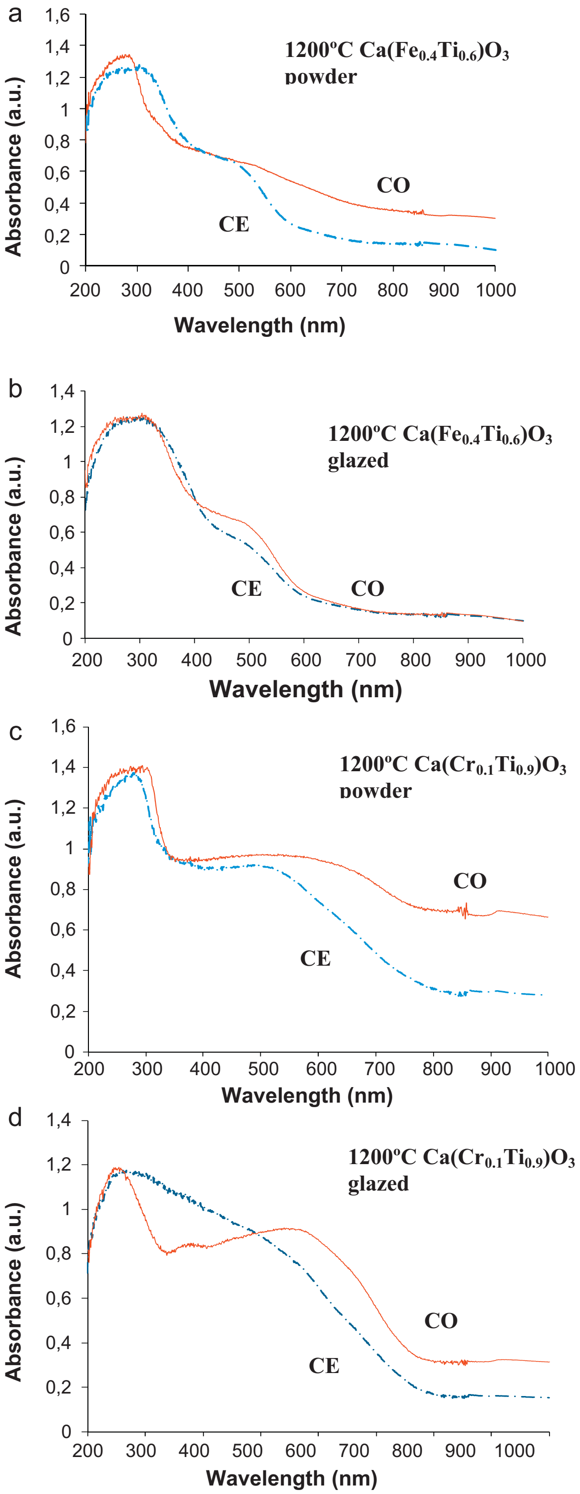

Fig. 5. UV–vis–NIR spectra of powders fired at 1200 °C and 5% glazed in a conventional CaO–ZnO–SiO$_2$ glaze in function of chromophore agent, temperature and synthesis method.

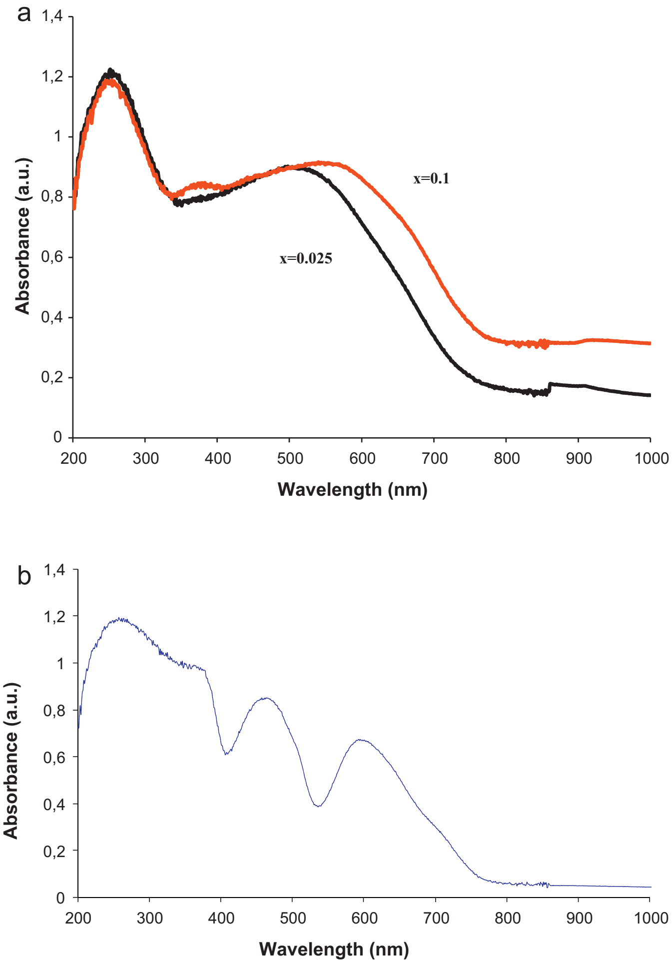

Fig. 6. UV–vis–NIR spectra: (a) powders CO Ca(Cr$_x$Ti$_{1-x}$)O$_3$ fired at 1200 °C and 5 wt.% glazed in a conventional CaO–ZnO–SiO$_2$ glaze and (b) 5% of eskolaite (Cr$_2$O$_3$) 5 wt.% glazed in a conventional CaO–ZnO–SiO$_2$ glaze.

The UV–vis–NIR of Ca(Cr$_x$Ti$_{1-x}$)O$_3$ powders that give pink shades in glazes ($x = 0.025$–0.1 for CE samples and $x = 0.025$–0.05 for CO samples all fired at 1200 °C) present a transfer band centred at 270 nm and a broad absorption in the visible range integrated by both bands at 370 and 520 nm (Fig. 5c CE). In the other hand the powders that give blue shades in glazes ($x = 0.2$ for CE samples and $x = 0.1$–0.2 for CO samples) present a transfer band centred at 270 nm and a broad absorption in the visible range integrated by three bands at 370, 500 and 600 nm (Fig. 5c CO).

The UV–vis–NIR of red-pink glazed samples of Ca(Cr$_x$Ti$_{1-x}$)O$_3$ ($x = 0.025$ and $x = 0.05$) fired at 1200 °C samples, show a transfer band centred at 250 nm and a broad absorption band that can be decomposed in two bands centred at 370 (weak) and 520 nm (strong) respectively (CO sample in Fig. 6) that can be assigned to Cr^{4+} in octahedral coordination [14]:

$$^3A_{2g}(F) \rightarrow {}^3T_{1g}(F)520\,\text{nm}.$$

$$^3A_{2g}(F) \rightarrow {}^3T_{1g}(P)370\,\text{nm}.$$

In the other hand, glazed blue shade obtained from $x = 0.1$ and 0.2 CO and $x = 0.2$ CE powders fired at 1200 °C and also from $x = 0.2$ CO sample at 1000 °C, show the transfer band at 250 nm and a broad absorption in the visible range that can be decomposed in three bands centred at 360, 500 and 600 nm respectively (Figs. 4a and 6). The additional absorption at

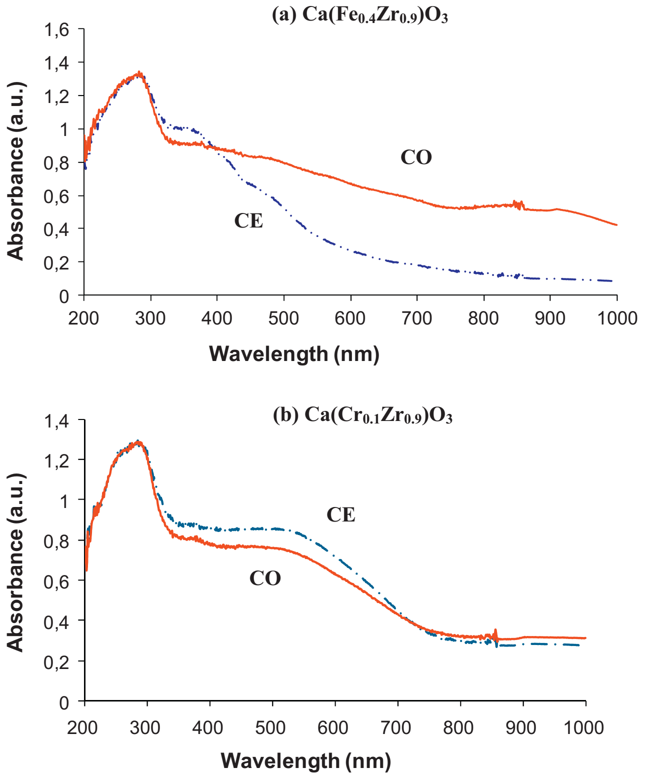

Fig. 7. UV–vis–NIR spectra of zirconate powders CO and CE fired at 1200 °C.

600 nm detected in high doped samples can be associated to transition $^4A_{2g} \rightarrow {}^4T_{2g}$ of Cr^{3+} in octahedral coordination (see Fig. 6b of glazed eskolaite). This absorption eliminates reflections in red wavelength range and glazed samples become bluish due to the minimum of absorption observed in the blue range (370–430 nm).

Therefore Cr^{4+} ion acts as red chromophore agent associated with 520 nm absorption band in red-pink samples but at higher x values (blue samples) Cr^{3+} ion entrance affects the color with its absorption at 600 nm (Fig. 6) [14,15]. The results indicate that both Cr^{4+} and Cr^{3+} enter in solid solution substituting Ti^{4+} into $CaTiO_3$ perovskite network, introducing oxygen vacancies in order to maintain the charge neutrality of the lattice.

SEM micrographs of pink powders $Ca(Cr_{0.025}Zr_{0.975})O_3$ fired at 1000 °C shown in Fig. 8 indicate that CO samples appear more monolithic and present higher particle size than CE samples. However the specific surface of these samples are similar: CE sample (5.02 m^2/g) slightly higher than CO sample (4.41 m^2/g).

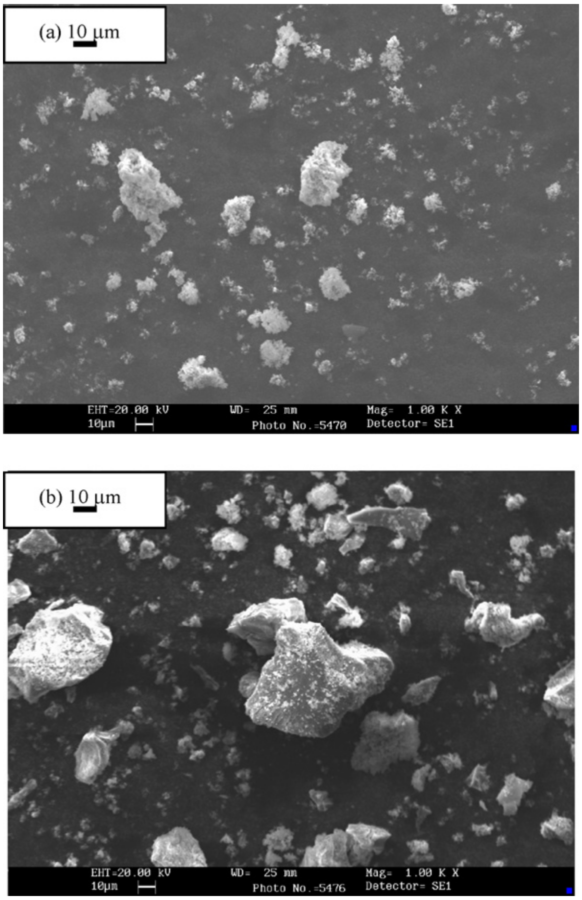

Fig. 8. SEM micrographs of samples $Ca(Cr_{0.025}Zr_{0.975})O_3$: (a) CE and (b) CO.

3.3. *Iron doped calcium titanate $Ca(Fe_xTi_{1-x})O_3$ with addition of 0.5 mol/mol of NH_4Cl*

$Ca(Fe_xTi_{1-x})O_3$ system crystallizes perovskite $CaTiO_3$ and pseudobrookite Fe_2TiO_5 together rutile as residual crystalline

Table 4
CIEL*a*b* parameters of powders fired at 1200 °C 5 wt.% glazed in a conventional CaO–ZnO–SiO_2 glaze in function of chromophore agent addition and synthesis method (in bold the best red-pink or blue colors obtained).

Sample	Method	$x = 0.2$	$x = 0.4$	$x = 0.6$	$x = 1$
$Ca(Fe_xTi_{1-x})O_3$	CE	73/12/18	74/10/28	68/12/22	65/11/19
	CO	**65/16/17**	71/14/31	71/13/32	59/11/13
$Ca(Fe_xZr_{1-x})O_3$	CE	85/2/18	81/2/25	71/5/21	68/7/27
	CO	84/2/20	78/5/24	69/7/23	**57/7/19**
Sample	Method	$x = 0.025$	$x = 0.05$	$x = 0.1$	$x = 0.2$
$Ca(Cr_xTi_{1-x})O_3$	CE	50/14/5	51/14/17	50/11/17	49/3/−3
	CO	**46/14/2**	45/11/4	44/6/−1	**45/3/−3**
$Ca(Cr_xZr_{1-x})O_3$	CE	79/−1/15	76/−1/16	68/−1/13	61/−2/10
	CO	77/−3/15	71/−3/14	69/−1/15	63/−2/12

phase, indicating that Fe–$CaTiO_3$ solid solution is not reached on these conditions (Table 2 and Fig. 2).

The UV–vis–NIR spectra of $Ca(Fe_xTi_{1-x})O_3$ powders show a transfer band centred at 300 nm due to iron–ligands interaction and a shoulder centred at 480 nm and a weak band at 880 nm for CE $x = 0.4$ sample at 1200 °C (Fig. 5a). A broad absorption in the visible range that can be decomposed in two bands centred at 480 and 650 nm respectively can be observed on Fig. 5a for CO $x = 0.4$ sample together the transfer band centred at 300. These bands can be associated to Fe^{3+} in octahedral coordination: 480 nm to $^6A_{1g} \rightarrow {}^4A_{1g}$, 650 nm to $^6A_{1g} \rightarrow {}^4T_{2g}$, and 880 nm to $^6A_{1g} \rightarrow {}^4T_{1g}$ [15–17]. When x increase (Table 4), the intensity of XRD peaks of pseudobrookite increase and the color of glazed samples change from a yellow shade (L*a*b* = 65/16/17 for CO $x = 0.2$ sample) at low x, to a pink color, decreasing all L*, a* and b* parameters (L*a*b* = 59/11/13 for CO $x = 1$ sample) associated with the presence of pseudobrookite.

3.4. Chromium doped calcium zirconate $Ca(Fe_xZr_{1-x})O_3$

$Ca(Cr_xZr_{1-x})O_3$ system crystallizes perovskite $CaZrO_3$ and zirconia (ZrO_2) in both monoclinic and cubic polymorphs. Likewise cubic form stabilises in higher intensity in CO samples (Table 1). Powders show a pink color in both CE (L*a*b* = 40/10/9 $x = 0.2$ at 1200 °C) and CO (L*a*b* = 41/9/10 $x = 0.2$ at 1200 °C) samples that are not stable in glazes producing green shades (Table 3 and Fig. 4b).

The UV–vis–NIR spectra of powders $x = 0.1$ fired at 1200 °C indicate that the red-pink color show a similar absorption pattern to chromium doped calcium titanate with a transfer band centred at 280 nm and a broad absorption in the visible range integrated by two bands at 380 and 510 nm associated to Cr^{4+} in octahedral coordination (Fig. 7b). The glazed samples $x = 0.2$ fired at 1000 °C indicates green color with absorption bands centred at 270, 450, 600 and 660 nm respectively (Fig. 4c), that can be assigned to Cr^{3+} in octahedral coordination (270 nm to $^4A_{2g} \rightarrow {}^4T_{1g}(P)$, 450 nm to $^4A_{2g} \rightarrow {}^4T_{1g}(F)$, 600 nm to $^4A_{2g} \rightarrow {}^4T_{2g}$ and 660 nm to $^4A_{2g} \rightarrow {}^2E_g$). It can be concluded that $Ca(Cr_xZr_{1-x})O_3$ solid solution is not reached completely in these samples: the limit of the solid solution of chromium in zirconium–calcium perovskite is lower than $x = 0.2$ and it are not stable in glazes, therefore it can not be considered a ceramic pigment.

3.5. Iron doped calcium zirconate $Ca(Fe_xZr_{1-x})O_3$

$Ca(Fe_xZr_{1-x})O_3$ system crystallizes perovskite $CaZrO_3$ and zirconia (ZrO_2) in both monoclinic and cubic polymorphs, as in the chromium doped calcium titanate system, but iron oxide is not detected in the samples. Cubic form stabilises in higher intensity in CO samples (Table 2). Powders show a light pink color in CE powders and more intense in CO powder (L*a*b* = 50/7/15 for CO $x = 0.2$ sample) but are not stable in glazes (Table 3).

The UV–vis–NIR spectra of powders $x = 0.4$ fired at 1200 °C (Fig. 7a) show a transfer band at 300 nm and bands centred at 350, 400 and 460 nm for CE sample and 400, 480, 650 and 850 nm for CO sample respectively. These bands can be associated to Fe^{3+} in octahedral coordination as has been discussed above (Section 3.3) [15]. The spectra of colorless glazed samples $x = 0.2$ fired at 1000 °C indicate the absence of color because only a transfer band centred at 300 nm can be observed (Fig. 4b). Therefore it can be concluded that $Ca(Fe_xZr_{1-x})O_3$ solid solution is not completely reached in these samples and is dissolved by glazes.

4. Conclusions

$Ca(Cr_xTi_{1-x})O_3$ $x = 0.025$, 0.05, 0.1 and 0.2 compositions obtained without addition of NH_4Cl as mineralizer, produce pink color in glazes at low x, but $CaCrO_4$ crystallizes when x increases, producing pin-hole defects and green colors in glazed samples. The crystallization of chromates can be avoided using NH_4Cl as mineralizer. Only chromium doped calcium titanate produce a complete solid solution in presence of NH_4Cl: the $Ca(Cr_xTi_{1-x})O_3$ titanate produces pink color in glazes at low x and dark blue shades at high x. CO samples produce blue colors at low x and at low temperature (1000 °C instead 1200 °C for CE sample). Cr^{4+} and Cr^{3+}, both in octahedral coordination, substitutes Ti^{4+} in titanate lattice. Cr^{4+} ion acts as the red chromophore agent associated with its 520 nm absorption band in red-pink samples, but at higher x values (blue samples), Cr^{3+} ion affects the color with its absorption at 600 nm.

Iron doped $Ca(Fe_xTi_{1-x})O_3$ system crystallizes perovskite $CaTiO_3$ and pseudobrookite Fe_2TiO_5 together with rutile as residual crystalline phase, indicating that Fe–$CaTiO_3$ solid solution is not completely reached on these conditions. Pseudobrookite increases with temperature and glazed samples change from a yellow to a pink color associated to pseudobrookite.

$Ca(Fe_xTi_{1-x})O_3$ and $Ca(Cr_xZr_{1-x})O_3$ system crystallizes perovskite $CaZrO_3$ and zirconia (ZrO_2) in both monoclinic and cubic polymorphs, but iron or chromium oxides are not detected in the powders. Cubic form stabilises in higher intensity in CO samples. The solid solutions is not reached completely in these samples and are not stable in glazes, therefore it cannot be considered ceramic pigments.

Acknowledgement

Authors acknowledge the financial support given by FUNDACION CAJA CASTELLÓN-UJI, P1-1B2010-09 project.

References

[1] (a) CPMA, Classification and Chemical Description of the Complex Inorganic Color Pigments, fourth ed., Dry Color Manufacturers Association, Alexandria, 2010;
(b) DCMA, Safe Handling of Color Pigments, Color Pigments Manufacturers Association Inc., 300 North Washington Street, Suite 102, Alexandria, 1993.

[2] R.A. Eppler, Black pigments free of heavy metals, US Patent 06/357959 (1983).

[3] F. Matteucci, C. Lepri Neto, M. Dondi, G. Cruciani, G. Baldi, A.O. Boschi, Colour development of red perovskite pigment $Y(Al,Cr)O_3$ in various ceramic applications, Adv. Appl. Ceram. 105 (2) (2006) 99–106.

[4] G. Monrós, M. Llusar, A. García, C. Gargori, R. Galindo, Development of new ceramic dyes, Adv. Sci. Technol. 68 (2010) 182–193.

[5] S. Kimura, A. Muan, Phase relations in the system CaO–iron oxide–titanium oxide under strongly reducing conditions, Am. Mineral. 56 (1971) 1347–1358.

[6] W.L. George, R.E. Grace, Formation of point defects in calcium titanate, J. Phys. Chem. Solids 30 (1969) 881–887.

[7] L.A. Dunyushkina, A.K. Demin, B.V. Zhuravlev, Electrical conductivity of iron-doped calcium titanate, Solid State Ion. 116 (1999) 85–88.

[8] A.A. Murashkina, A.N. Demina, Doping of calcium titanate with chromium and indium, Inorg. Mater. 41 (4) (2005) 402–405.

[9] C. Gargori, S. Cerro, R. Galindo, A. García, M. Llusar, J. Badenes, G. Monrós, New vanadium doped calcium titanate ceramic pigment, Ceram. Int. 37 (2011) 3665–3670.

[10] C. Gargori, R. Galindo, M. Llusar, S. Cerro, A. García, G. Monrós, Chromium–calcium titanate red ceramic pigment, Adv. Sci. Technol. 68 (2010) 208–212.

[11] G. Pfaff, Synthesis of calcium titanate powders by sol–gel process, Chem. Mater. 6 (1994) 58–62.

[12] CIE Commission International de l'Eclairage, Recommendations on Uniform Color Spaces, Color Difference Equations, Psychometrics Color Terms. Supplement no. 2 of CIE Pub. No. 15 (E1-1.31) 1971, Bureau Central de la CIE, Paris (1978).

[13] S. Brunauer, P.H. Emmett, E. Teller, Adsorption of gases in multimolecular layers, J. Am. Chem. Soc. 60 (1938) 309–319.

[14] G. Monrós, H. Pinto, J. Badenes, M. Llusar, M.A. Tena, Chromium(IV) stabilisation in new ceramic matrices by coprecipitation method: application as ceramic pigments, Z. Anorg. Allg. Chem. 631 (2005) 2131–2135.

[15] A.B. Lever, Studies in Physical and Theoretical Chemistry Inorganic Electronic Spectroscopy, vol. 3, Elsevier, Amsterdam, 1986.

[16] A. Garcia, M. Llusar, J. Badenes, M.A. Tena, G. Monrós, Encapsulation of hematite in zircon by microemulsion and sol–gel methods, J. Sol–Gel Sci. Technol. 27 (2003) 267–275.

[17] A. Khaleel, Sol gel synthesis, characterization and catalytic activity of Fe(III) titanates, Colloids Surf. A: Physicochem. Eng. Aspects 346 (2009) 130–137.